Comparative Study of the Resolution of Ge-on-Si Photodetectors for 1μ m Infrared Signals

Jahangiri, Mojtaba; Sberna, Paolo; Sammak, Amir; Nihtianov, Stoyan

DOI
10.1109/ONCON56984.2022.10126983

Publication date
2022

Document Version
Final published version

Published in
1st IEEE Industrial Electronics Society Annual On-Line Conference, ONCON 2022

Comparative Study of the Resolution of Ge-on-Si Photodetectors for 1 μm Infrared Signals

1st Mojtaba Jahangiri
Department of Microelectronics,
Faculty of Electrical Engineering, Mathematics, and Computer Science
Delft University of Technology
Delft, The Netherlands
m.jahangiri@tudelft.nl

2nd Paolo Sberna
Department of Microelectronics,
Faculty of Electrical Engineering, Mathematics, and Computer Science
Delft University of Technology
Delft, The Netherlands
p.m.sberna@tudelft.nl

3rd Amir Sammak
QuTech and
Netherlands Organization for Applied Scientific Research (TNO)
Delft, The Netherlands
amir.sammak@tno.nl

4th Stoyan Nihtianov
Department of Microelectronics,
Faculty of Electrical Engineering, Mathematics, and Computer Science
Delft University of Technology
Delft, The Netherlands
s.nihtianov@tudelft.nl

2022 IEEE 1st Industrial Electronics Society Annual On-Line Conference (ONCON) | 979-8-3503-9806-9/22/$31.00 ©2022 IEEE | DOI: 10.1109/ONCON56984.2022.10126983

***Abstract*— Most of the studies on narrow-band near-infrared detection reported so far are related to the 1.3 μm and 1.55 μm spectral windows. There is insufficient research work done on radiation detection in the narrow band around 1 μm wavelength, which is just outside the Si (0.95 μm) and GaAs (0.85 μm) effective cut-off spectral sensitivity. This paper presents a p^+n Ge-on-Si detector with a customized large active window, employing the PureGaB technology, to detect radiation in a very narrow band around 1 μm. The advantages of the proposed detector are: (1) CMOS-compatibility and micro-spectroscopic capability; (2) low dark current and high photoresponsivity, compared to similar devices reported in the literature; (3) enhanced sensitivity to weak radiation by realizing an ultra-shallow and very thin depletion region. These detectors can be good candidates for measuring the YAG laser radiation and measuring stray radiation in photolithography.**

Keywords*— *Infrared detection, SiGe Junction, Ge-on-Si Photodiode, 1-μm Infrared;

I. INTRODUCTION

Most narrow-band detectors in the near-infrared region have been developed for two commercially used optical windows:1.3 μm and 1.55 μm. Applications which demand these spectral windows are: fiber optics and LIDAR technology [1][2]. At the same time, detecting and accurately measuring weak radiation in a narrow spectrum around 1 μm can be very helpful for specific applications such as photolithography and YAG lasers [3].

Knowledge of the radiation power of possible unwanted spectral components of a photolithography exposure beam plays an important role for the accurate transfer of a pattern from a mask to a photosensitive substrate. An ideal exposure beam should be free of out-of-band spectral components [4]. However, the existing technologies for producing high-power deep/extreme ultraviolet radiation produce also unwanted out-of-band radiation, which should not be allowed to enter the illumination and projection optics. Unfortunately, the removal of these spectral components is not always 100% efficient. So, identifying and measuring these components, superimposed on powerful deep/extreme ultraviolet radiation, is important, but also very challenging. Some of the unwanted spectral components are in the near-infrared (NIR) spectrum [5]. A NIR spectrum below 950 nm is relatively easily absorbed in silicon. Therefore, silicon detectors with a well-designed depletion region and a UV/visible blocking filter can offer a relatively good solution for the infrared spectral range from 750 nm to 950 nm. Above this spectrum the sensitivity of the silicon detectors drops very quickly, especially when their depletion region cannot be very wide. That is why for the NIR spectrum above 950 nm, photodetectors based on narrow bandgap semiconductors, such as germanium or InGaAs, are preferred.

In this paper we present a CMOS-compatible SiGe NIR detector for the narrow spectral range from 950 nm to 1150 nm, with sufficient responsivity and good noise equivalent power (NEP). The detector is produced using the so called PureGaB process, which provides a very shallow junction when gallium/boron passivation capping layer is deposited on n-doped germanium, using chemical vapor deposition (CVD) [6]. We provide a comparison of the measured performance of two detectors: a silicon detector produced with the PureB process and a SiGe detector produced with the PureGaB process. The only difference between the two processes is the presence of gallium in the capping layer when the substrate is germanium [6]. Furthermore, the spectral responsivity of the customized SiGe photodetector is simulated with an integrated bandpass filter, providing: (1) maximized sensitivity close to the 1 μm wavelength and (2) efficient blocking of ultraviolet radiation. We then compare the performance of the new detector with state-of-the-art devices reported in the literature, demonstrating its competitiveness (dark current density, photoresponsivity, noise equivalent power).

Section II presents the design approach and the fabrication method of the SiGe photodetector. In Section III, we compare the properties of the SiGe detector with the Si photodetector and highlight the property variation trend when varying the $Si_{1-x}Ge_x$ composition ratio. Finally, we compare the resolution of the proposed SiGe device with SiGe devices reported in the literature. Section IV summarizes the achieved results.

II. Design Approach and Fabrication Method

Considering the lattice mismatch between Si and Ge crystals, growing germanium over a silicon substrate can influence the quality of the germanium epitaxial layer in terms of defects and discontinuity. To solve this issue, the double temperature growth technique and a gradual increase of the germanium content in the Si/Ge epitaxial layer were used. The PureGaB process provides a radiation-hard interface with germanium, in addition to the extremely shallow depletion region [7] [8].

A. Device fabrication

A simplified vertical stack of the processed devices is shown in Figure 1. The substrate was an n-type silicon wafer with <100> orientation and resistivity of 1-5 Ω.cm. The device fabrication approach was to first create the passivation oxide layer, and next to open the windows in the oxide layer to grow the germanium epitaxial layers. In Figure 1, the following processing steps are presented: (a) a 10 µm epitaxial low-doped n-Si layer (in yellow) was grown over an n^+ buried layer (in brown) by an ASMI Epsilon 2000 CVD epitaxial growth machine; (b) a 2 µm oxide layer (in purple) was grown; (c) n+ dopant wells (in brown) were implanted on both the backside and the front side of the wafer, and p+ dopant wells (in blue) were planted on the frontside side; (d) the oxide was removed using a photoresist mask by first plasma dry etching followed by wet etching with a soft landing on Si. Next, HF deep etching and the Marangoni drying method were applied to create a clean opening on the Si surface without any dangling bonds, allowing the growth of high-quality epitaxial layers. Using the ASMI Epsilon 2000 CVD epitaxial growth reactor, a low-doped $Si_{1-x}Ge_x$ composition (in light green) with a thickness of 2 µm was grown selectively on silicon. Next, without breaking the high vacuum, a 10-nm PureGaB capping passivation layer (in darker green) was epitaxially grown [9]; (e) surface metallization was done (in gray) with 1 µm Al/Si (1%) thin films through RF sputtering at 350˚C and 400W RF power; (f) finally, an open window was created for the active area of the photodetector by etching the metal layer, followed by deposition of an integrated optical filter stack over the whole die surface, and then removed from the area outside the active photodetector area.

B. Doping consideration

The following doping levels were used for the different device layers:

Layer	Doping level (atoms/cm^2)
Substrate (Phosphorus)	9.2E+14 ~ 5.0E+15 <n-type>
Epitaxial low-doped silicon (Arsenic)	1.97E+15
Initial buried layer (Arsenic)	1.0E+17
n^+ doped layer (Phosphorus)	5.0E+15
p^+ doped layer (Boron)	1.0E+13
Ge layer (Arsenide)	~ 2.0E+15

In the capping GaB layer, Ga and B were 1 nm and 10 nm thick, respectively.

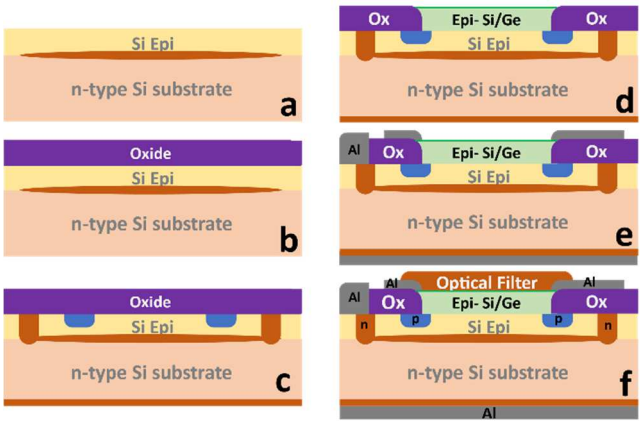

Fig. 1. Device vertical stack and fabrication process steps: (a) low-doped epitaxial silicon growth, (b) field oxide growth, (c) ion implantation to create guard rings and channel stops, (d) engineered epi-growth of Si/Ge layer (in light green) and a thin PureB/PureGaB passivation layer (in dark green), (e) metalization, and (f) optical thin-film stack deposition.

C. Integrated optical window

A narrow spectral responsivity is achieved by using an optical filter on top of the detector active surface. In the targeted application, the detector has to ignore radiation with a spectrum above 1150 nm. In addition to the role of the filter, the reduction of the sensitivity to longer wavelengths is achieved by engineering the depth and width of the depletion region of the detector. Two options for an optical bandpass filter were considered for the absorption or reflection of the shorter out-of-band wavelengths (Figure 2). Option 1: a quad-layer stack of Si/SiO_2 with a total thickness of 1140 nm, and Option 2: a bilayer stack of $GaAs/SiO_2$ with a total thickness of 495 nm. Both filters can be integrated on the detector surface. Figure 2 shows the simulated transmittance of photons through the two types of filters in a wider spectrum. It was observed that both filters can absorb or reflect all radiation wavelengths lower than 400 nm and reach a transmittance peak at 1030 nm. Although Option 2 shows a sharper peak at 1 µm, lower profile thickness, and lower transparency in the visible region, the challenges with the deposition and the integration of a GaAs layer using CMOS technology led to the selection of Option 1 as the preferred choice.

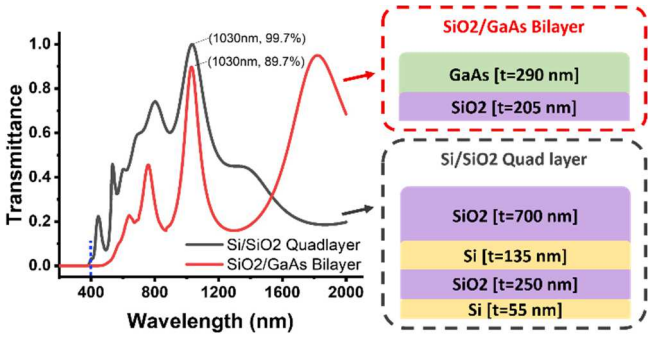

Fig. 2. Optical response (transmittance) of two options proposed as 1 µm bandpass filters for high transmission of 950 nm to the 1150 nm narrow band.

III. Results and Discussion

The "OpenFilter" software of "Ecole Polytechnique de Montreal, Canada" was used to design the optical bandpass filters with an optimized stack and absorption profile. The presented Quantum efficiency of the device is the product of the optical filter's transmittance profile and the Si/Ge absorption profile. The electrical measurements were performed by a cascade probe station and Keysight B1500A Semiconductor Device Analyzer in no light condition (Dark-mode) with the help of IC-CAP 2020 software.

Increasing the thickness of the epi-Ge layer on the silicon substrate raises the chance of an increased number of defects and dislocations in the crystallography of the device and a non-uniform thickness of the layer. To determine the minimum required Ge thickness in a Ge-on-Si photodetector for application in the near-infrared band around 1 µm wavelength, we studied the attenuation profile of a 1 µm photon beam in Ge and compared it with the attenuation profile in Si. Figure 3A illustrates the attenuation of the 1 µm photon beam into Ge and Si as a function of the absorbing layer thickness. It can be seen that the beam can be almost fully absorbed in the first ~2 µm of the Ge layer, while it does not show even minor absorption (< 3%) in the 10 µm silicon layer. Therefore, Ge thickness of 2 um was chosen for further investigation. The green highlighted area in Figure 3A presents the absorption in a SiGe alloy with an arbitrary ratio between the Si and Ge content: $Si_{1-x}Ge_x$, with 0<x<1.

From Figure 3A, we see that using Ge improves the 1 µm wavelength photon absorption in a relatively small layer thickness, leading to a stronger photogeneration current and higher quantum efficiency and photoresponsivity. However, compared with Si, using Ge leads to an increased dark current due to the lower bandgap of Ge. Figure 3B illustrates the variation of the dark current (green highlighted area) from approximately 10^{-11} A (x=1: Si) to 10^{-7} A (x=1: Ge) in a $Si_{1-x}Ge_x$ epi-layer for a detector occupying a 1.75 mm^2 area (this particular area is related to a specific application), corresponding to 1.3 x 10^{-17} A/µm^2 and 4.0 x 10^{-13} A/µm^2 current densities, respectively.

It is important to point out that the photodetector resolution is inversely proportional to the square root of the dark current level (due to the associated shot noise) and is proportional to the responsivity:

$$\uparrow Resolution \equiv \downarrow Dark\ Current\ \&\ \uparrow Spectral\ Responsivity$$

Figure 3C presents the simulation results of the proposed photodetectors' quantum efficiency (QE) with an integrated Si/SiO_2 quad-layer optical filter. From the results of the quantum efficiency, the spectral responsivity can be calculated using the expression:

$$Spectral\ responsivity\ \left(\frac{A}{W}\right) = QE \times \frac{q}{h.f} = QE \times \frac{\lambda\,(nm)}{1240} \quad (1),$$

where q is the electron charge, f is the photon frequency, h is Plank's constant, and λ is the photon wavelength in nm [10].

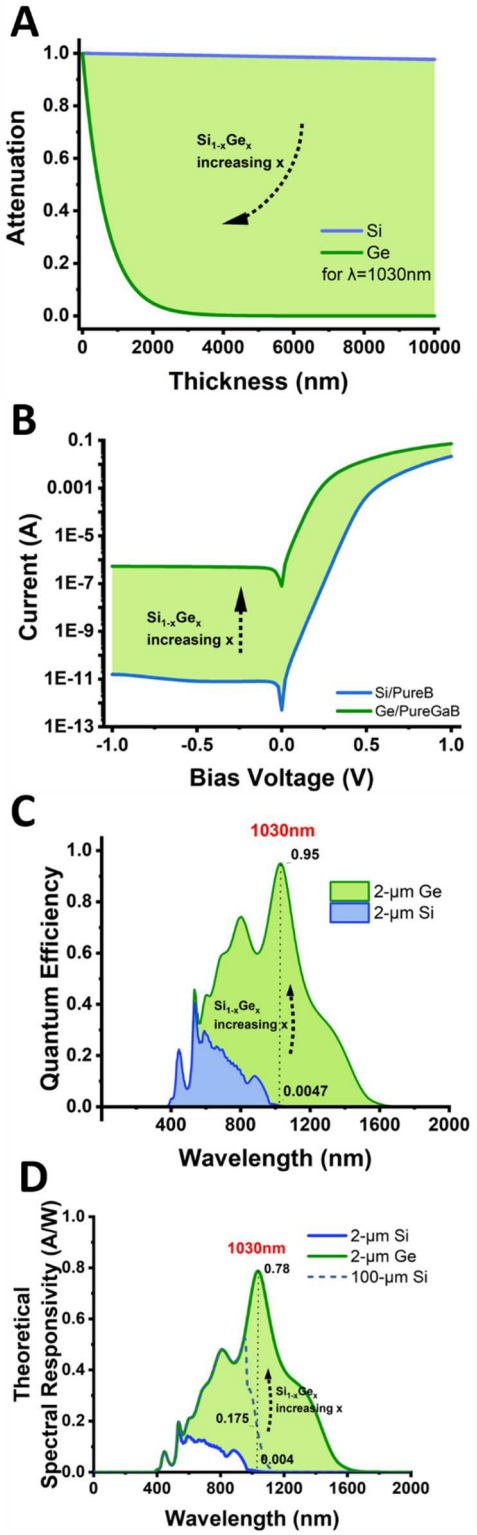

Fig. 3. The trend of the $Si_{1-x}Ge_x$ photodetector's property changes by x% of Ge in the SiGe alloy. (A) Comparison of the 1 µm wavelength absorption profiles of Si and Ge as a function of thickness. (B) Comparison of the dark current of the PureB/Si and PureGaB/Ge detectors. (C) Quantum efficiency of the PureB/Si and PureGaB/Ge detectors with the Si/SiO_2 quad-layer optical filter. (D) Theoretical spectral responsivity of the PureB/Si and PureGaB/Ge detectors with the Si/SiO_2 quad-layer optical filter and 2 µm depletion width. The dashed line is shown the theoretical spectral responsivity of the PureB/Si detector with 100 µm depletion layer width.

Figure 3D shows the spectral photoresponsivity achieved by the PureB/Si and PureGaB/Ge detectors with 2 µm depletion width when a Si/SiO2 quad-layer optical filter is

integrated on their surface. At 1 µm wavelength the responsivity of the SiGe detector is 0.78 A/W, while for silicon with the same depletion layer width the responsivity is only 0.004 A/W. Of course, increasing the depletion width of the silicon detector will improve its responsivity. For comparison, the dashed line in Figure 3D shows the theoretical spectral responsivity of the PureB/Si detector with a 100 µm depletion layer. The responsivity of this detector at 1 µm is increased up to about 0.2 A/W, which is only 4 times less than the Ge detector. However, realizing such a wide depletion region requires either the use of special wafers or building thick high-quality epitaxial layers. Although technologically it is possible to create a low-doped silicon epi layer with large thicknesses, this is not part of the standard CMOS processes.

IV. Comparative Study of SiGe NIR Detectors

TABLE 1. COMPARATIVE TABLE OF RECENTLY REPORTED INFRARED SIGE PHOTODETECTORS

N	Type of Device	SiGe Structure		Dark Current Density (A/µm²)	Measured Spectral Range (nm)	Photo Responsivity (A/W)	NEP* at 1µm² (W/µm²)	Application	Ref.
1	21-GHz-Bandwidth Germanium-on-Silicon Photodiode	n^+-Si sub / 0.18 µm $Si_{0.58}Ge_{0.42}$/ 0.28 µm $Si_{0.42}Ge_{0.58}$/ 1.7 µm Ge		1.0×10^{-9} @-1V	@ 1.3 µm	0.4 ~ 0.6	1.6~3 E-9	RF bandwidth–efficiency optoelectronics	2006 [11]
					@ 1.55 µm	0.28			
2	SiGe Buffer Layers in Reducing Dark Currents of Ge-on-Si Photodetectors	n^+-Si sub / 0.4 µm $Si_{0.5}Ge_{0.5}$/ 0.7 µm $Si_{0.40}Ge_{0.60}$/ 2.6 µm Ge		5×10^{-11} @-1V	@ 1.3 µm	0.53	1 E -12	High-speed optoelectronics	2007 [12]
3	Ge/SiGe Multiple Quantum Well	vertical p-i-n 20 QW of Ge/ $Si_{0.15}Ge_{0.85}$ sandwiched by $Si_{0.1}Ge_{0.9}$		1.6×10^{-9} @-1V	1400 to 1440 nm	0.03 ~ 0.05	3.2~5.3E-8	30GHz bandwidth optoelectronics	2011 [13]
4	High Performance of an SOI-based Lateral PIN Photodiode	SiGe/Si multilayer quantum well heterojunction		~1.0×10^{-13} @-1V	400 to 1600 nm	~0.87 @-3V	~1.1E-13	High-performance photodiode	2012 [14]
5	SiGe Quantum Dots Over Si Pillars	$Si_{0.3}Ge_{0.7}$ QDs over array of p+-Si nanopillars (Si pillar/ $Si_{0.3}Ge_{0.7}$ QD/ ITO)		3.0×10^{-16} @-0.5V	600 to 1600 nm	$\frac{photocurrent}{dark\ current}$ 400 @ 1 µm	NA	Optical interconnects telecommunications	2013 [15]
6	SiGe-based pin near-infrared photodetectors	p^+- Si/p^+- $Si_{0.7}Ge_{0.3}$/ i- $Si_{0.5}$ $Ge_{0.5}$/ n^+-$Si_{0.4}Ge_{0.6}$/ n^+-aSi		NA	1450 to 1650 nm	0.35	NA	CMOS-compatible infrared detection	2014 [16]
7	Strain-balanced Si/SiGe type-II superlattices	Epitaxial type-II heterostructure of alternating Si and SiGe alloys on $Si_{0.83}Ge_{0.17}$ relaxed buffer layers	$Si_{0.46}Ge_{0.54}$	2.8×10^{-13}	1100 to 1700 nm Measured data of 1320 nm @ -4V	1.55E-4	1.8E-9	Near-infrared photodetection	2014 [17]
			$Si_{0.39}Ge_{0.61}$	3.4×10^{-13}		2.52E-4	1.3E-9		
			$Si_{0.28}Ge_{0.72}$	2.7×10^{-13}		1.76E-4	1.5E-9		
			$Si_{0.23}Ge_{0.77}$	8.0×10^{-13}		1.72E-4	4.6E-9		
8	Integrated SiGe Detectors for Si Photonic	Ge-on-Si on 3-µm Oxide		4×10^{-12}	@ 1.3 µm	0.2	2E-11	Si photonic sensor platforms	2017 [18]
9	SiGe nanocrystals in SiO_2	Sputtered SiGe-NCs:SiO2/SiO2/Si	$Si_{25}Ge_{25}$:50%SiO_2	3.0×10^{-16} @-1V	@ 1 µm	~2.2	1.3E-16	Hybrid devices	2020 [19]
			Si_5Ge_{45}:50%SiO_2			~1	3E-16		
10	Si/Ge/Si photodiodes	Si/Ge/Si		4.8×10^{-9} at -1V	N/A	0.81	5.9 E -9	High-speed integrated waveguide	2020 [20]
11	Ge PIN photodetectors	Si Sub/Ge Buffer/p^+-Ge/i-Ge/n^+-Ge		5×10^{-11}	@ 1.55 µm	0.12	4.1 E -10	Detection of 1.55 µm wavelength	2020 [21]
12	Ge-on-Si CMOS compatible for 1 µm wavelength	Ultra-large area Ge-on-Si (PureGaB/ 2µm Epi-Ge/ Si)		4×10^{-13} @-1V	@1 µm	~ 0.7 to 0.8 (Simulated)	5~5.7 E-13	Weak 1µm infrared radiation detection	**This Paper**
	Si-on-Si CMOS compatible for 1 µm wavelength	Ultra-large area Si-on-Si (PureB/ 10µm Epi-i-Si / Si)		1.33×10^{-17} @-1V	@1 µm	~ 4.0E-3 (Simulated)	~3.3 E-15	Weak 1µm infrared radiation detection	

** Lower brings better SNR*

Table 1 presents recently reported (since 2006) near-infrared SiGe photodetectors in scientific publications, with their Dark Current Density, Spectral Range, Photoresponsivity, and Noise Equivalent Power (NEP) for a 1µm² area. Columns 2 to 8 present: the type of studied device: a simple structure of fabricated SiGe region: dark current density: reported spectral range in the study: photoresponsivity in the reported spectrum or specified wavelength: calculated noise equivalent power based on equation 2: potential application proposed in the references.

The devices presented in Table 1 have a variety of different structures: 1) an epitaxially grown SiGe layer with three fixed Ge:Si ratios (N6); 2) an epitaxially grown SiGe layer by gradually increasing the Ge content (N1); 3) epitaxially grown pure Ge (N8); 4) a Si-Ge-Si layer (N10); 5) a $Si_{1-x}Ge_x$ quantum well sandwich (N3); 6) $Si_{1-x}Ge_x$ nanocrystal growth through sputtering (N9); 7) a SiGe/Si Multilayer Heterojunction (N4).

Most reported optical applications in Table 1 are in the 1.3 µm and 1.55 um spectrum. Unfortunately, we could not

find an IR detector optimized explicitly for the 1 μm spectrum.

It can be inferred from Table 1 that the most advanced Ge-based photodetectors would have a dark current density in the order of 10^{-11}~10^{-13} A/μm^2, while good quality Si-based photodiodes have a dark current density in the order of 10^{-17}~10^{-18} A/μm^2. Photodetectors based on a $Si_{1-x}Ge_x$ alloy will have dark current densities between 10^{-11}~10^{-13} A/μm^2 and 10^{-17}~10^{-18} A/μm^2.

A good criterion for comparing the performance of different photodetectors is the Noise Equivalent Power (NEP) [22][23]:

$$NEP = \frac{I_{Dark\ Current}\ (A/\sqrt{Hz})}{Spectral\ responsivity(A/W)} \quad (2)$$

NEP has an inverse relationship with the signal-to-noise ratio (SNR):

$$SNR = \frac{Illumination\ Signal\ Power}{Noise\ Equivalent\ Power} (3)$$

For a given radiation power, lower NEP provides a higher photodetector SNR, resulting in a better accuracy. The ideal photodetector for 1 μm radiation would be the one with the highest spectral responsivity and lowest dark current. The fabricated Ge/PureGaB photodetector has a photoresponsivity of 0.78 A/W at 1 μm and a dark current of 4.0E^{-13} A/μm^2 (NEP ~5.13E^{-13} W/μm^2). Compared to the photodetectors presented in Table 1, the proposed detector can be considered a very good option for the near-infrared spectrum, tuned explicitly for 1 μm radiation.

V. Conclusion and Future Work

A Ge-on-Si-based photodiode is proposed with an optical filter to detect weak 1 μm wavelength radiation. The photodiode is processed and its electrical characteristics measured, while at this point, the optical filter is only designed and its optical characteristics simulated. The photodetector demonstrates high sensitivity, very good ultraviolet blindness, and a relatively low dark current. The relatively thin depletion region requiring no or low reverse bias voltage makes this photodetector attractive for microspectrometric devices to distinguish the 1 μm beam component. In addition, the PureB/GaB technology provides an opportunity of creating a shallow depletion region (extending almost from the surface). The proposed optical filter increases the detector's selectivity by blocking 99.9% of wide-range ultraviolet radiation. The joint detector + filter suppression of longer infrared radiation above 1.6 μm is 98.9%, while reaching 95% transparency at 1 μm wavelength.

Comparing the NEP of the Ge/PureGaB photodetector and the Si/PureB detector with the same depletion width shows that the Ge/PureGaB photodetector has two orders higher NEP, which may be considered as a disadvantage. However, at the same time the Ge/PureGaB photodetector provides more than 200 times stronger output photocurrent and 2 times better SNR for the same radiation intensity, which in most applications is the preferred option.

Potential applications of the proposed detector are: (1) measuring YAG laser radiation at 1 μm, (2) in portable/ micro-spectrometric devices to distinguish the 1 μm beam component in wide spectrum radiation, (3) CMOS-compatible photodetector's array implemented on chips, (4) measuring stray radiation in photolithography.

The next step is to integrate the optical filter with the photodiode and to prove the optical characteristics of the selective IR detector experimentally.

Acknowledgment

This work is supported by the European project PIn3S.

References

[1] J. Michel, J. Liu, and L. C. Kimerling, "High-performance Ge-on-Si photodetectors," *Nat. Photonics*, vol. 4, no. 8, pp. 527–534, 2010, doi: 10.1038/nphoton.2010.157.

[2] M. Vollmer, K.-P. Möllmann, and J. A. Shaw, "The optics and physics of near infrared imaging," in *Education and Training in Optics and Photonics*, 2015, p. TPE09.

[3] M. Fujiwara, H. Hamaguchi, and M. Tasumi, "Measurements of Spontaneous Raman Scattering with Nd:YAG 1064-nm Laser Light," *Appl. Spectrosc.*, vol. 40, no. 2, pp. 137–139, Feb. 1986.

[4] V. Bakshi, *EUV Lithography*. SPIE Press, 2018.

[5] T. Knežević, M. Krakers, and L. K. Nanver, "Broadband PureGaB Ge-on-Si photodiodes responsive in the ultraviolet to near-infrared range," in *Optical Components and Materials XVII*, 2020, vol. 11276, pp. 73–85, doi: 10.1117/12.2546734.

[6] A. Sammak, "Silicon-based integration of groups III, IV, V chemical vapor depositions in high-quality photodiodes," 2012.

[7] L. Shi and S. Nihtianov, "Comparative study of silicon-based ultraviolet photodetectors," *IEEE Sens. J.*, vol. 12, no. 7, pp. 2453–2459, 2012.

[8] A. Sammak, L. Qi, W. B. de Boer, and L. K. Nanver, "PureGaB p+ n Ge diodes grown in large windows to Si with a sub-300 nm transition region," *Solid. State. Electron.*, vol. 74, pp. 126–133, 2012.

[9] L. Marković, T. Knežević, L. K. Nanver, and T. Suligoj, "Modeling and Simulation Study of Electrical Properties of Ge-on-Si Diodes with Nanometer-thin PureGaB Layer," in *2021 44th International Convention on Information, Communication and Electronic Technology (MIPRO)*, 2021, pp. 64–69, doi: 10.23919/MIPRO52101.2021.9597002.

[10] M. Bass *et al.*, *Handbook of Optics, Third Edition Volume II: Design, Fabrication and Testing, Sources and Detectors, Radiometry and Photometry*. McGraw Hill LLC, 2009.

[11] Z. Huang *et al.*, "21-GHz-Bandwidth Germanium-on-Silicon Photodiode Using Thin SiGe Buffer Layers," *IEEE J. Sel. Top. Quantum Electron.*, vol. 12, no. 6, pp. 1450–1454, 2006, doi: 10.1109/JSTQE.2006.884073.

[12] Z. Huang, J. Oh, S. K. Banerjee, and J. C. Campbell, "Effectiveness of SiGe buffer layers in reducing dark currents of Ge-on-Si photodetectors," *IEEE J. Quantum Electron.*, vol. 43, no. 3, pp. 238–242, 2007.

[13] P. Chaisakul *et al.*, "Ge/SiGe multiple quantum well photodiode with 30 GHz bandwidth," *Appl. Phys. Lett.*, vol. 98, no. 13, p. 131112, 2011.

[14] P. S. Menon, S. K. Tasirin, I. Ahmad, and S. F. Abdullah, "High performance of a SOI-based lateral PIN photodiode using SiGe/Si multilayer quantum well," in *2012 10th IEEE International Conference on Semiconductor Electronics (ICSE)*, 2012, pp. 403–406, doi: 10.1109/SMElec.2012.6417172.

[15] W.-T. Lai, P.-H. Liao, A. P. Homyk, A. Scherer, and P.-W. Li, "SiGe Quantum Dots Over Si Pillars for Visible to Near-Infrared Broadband Photodetection," *IEEE Photonics Technol. Lett.*, vol. 25, no. 15, pp. 1520–1523, 2013, doi: 10.1109/LPT.2013.2270281.

[16] J. W. Zeller *et al.*, "Design and development of SiGe based near-infrared photodetectors," in *Infrared Sensors, Devices, and Applications IV*, 2014, vol. 9220, pp. 48–55.

[17] D. Ali and C. J. K. Richardson, "Strain-balanced Si/SiGe type-II superlattices for near-infrared photodetection," *Appl. Phys.*

Lett., vol. 105, no. 3, p. 31116, Jul. 2014, doi: 10.1063/1.4891172.

[18] G. Pandraud, S. Milosavljevic, A. Sammak, M. Cherchi, A. Jovic, and P. Sarro, "Integrated SiGe Detectors for Si Photonic Sensor Platforms," *Proceedings*, vol. 1, no. 4. 2017, doi: 10.3390/proceedings1040559.

[19] I. Stavarache *et al.*, "SiGe nanocrystals in SiO2 with high photosensitivity from visible to short-wave infrared," *Sci. Rep.*, vol. 10, no. 1, p. 3252, 2020, doi: 10.1038/s41598-020-60000-x.

[20] H. Zegmout *et al.*, "High speed integrated waveguide lateral Si/Ge/Si photodiodes with optimized transit time," in *Silicon Photonics XV*, 2020, vol. 11285, pp. 188–195.

[21] X. Zhao *et al.*, "Design impact on the performance of Ge PIN photodetectors," *J. Mater. Sci. Mater. Electron.*, vol. 31, no. 1, pp. 18–25, 2020, doi: 10.1007/s10854-018-00650-w.

[22] V. Mackowiak, J. Peupelmann, Y. Ma, and A. Gorges, "NEP–noise equivalent power," *Thorlabs, Inc*, vol. 56, 2015.

[23] P. L. Richards, "Bolometers for infrared and millimeter waves," *J. Appl. Phys.*, vol. 76, no. 1, pp. 1–24, Jul. 1994, doi: 10.1063/1.357128.